Borneo Journal of Resource Science and Technology (2022), 12(1): 106-124
DOI: https:doi.org/10.33736/bjrst.4261.2022

Multi-Stimuli-Responsive Organogel Based on Bisthiourea Compounds for The Removal of Selected Organic Dyes

FARIS-DANISH YUSAINI & MAYA-ASYIKIN MOHAMAD ARIF*

Faculty of Resource Science and Technology, Universiti Malaysia Sarawak, 94300 Kota Samarahan, Sarawak, Malaysia
*Corresponding author: mamasyikin@unimas.my
Received: 29 November 2021 Accepted: 10 February 2022 Published: 30 June 2022

ABSTRACT

The self-assembly of a series of bisthiourea containing amino acid side chains has been studied in a large range of organic solvents. Self-assembly is driven mainly by hydrogen bonding groups of thiourea and amino acids moieties. Of all the synthesized compounds, only bisthiourea with alanine side chains, **3.5** formed thermoreversible gel in 50:3 dichloromethane:water mixture at minimum gel concentration of 0.5%. SEM micrographs of the gel showed the formation of entangled cross-linked fibres. The addition of anions such as Cl^-, F^- and AcO^- disrupted the gel network of **3.5** thus inducing the gel-sol transition. To investigate the ability of the bisthiourea to form metallogel, metal ions such as Co^{2+}, Cu^{2+}, Ni^{2+} and Pb^{2+} were introduced, however, none of them induce the formation of metallogel. In particular, the gels show good performance in the absorption of bromocresol green and Eriochrome black-T at 75% and 61% efficiency, respectively within 24 hours. The good dye absorption properties of gel **3.5** render the potential of bisthiourea gels as new dye absorption materials, which show significant benefit for water pollution treatment.

Keywords: Anion responsive, bisthiourea derivatives, organic dyes removal

INTRODUCTION

Supramolecular gels are viscoelastic materials that are made of small amount of gelators and large volume of solvents (Dastidar & Mondal, 2018). The formation of the gels, solid-like materials are due to the surface tension or capillary force action of the immobilized solvents. Supramolecular gels are formed through numerous supramolecular (noncovalent) interactions such as hydrogen bonding, π-π stacking, van der Waals interactions, halogen interaction, and charge transfer interactions which contribute to the tunable properties of the gel. In contrast, chemical or polymer gel such as silica gels are formed through covalent interactions, thus are not readily tunable as it requires a significant amount of energy to break the bond (Dastidar *et al.*, 2016). The supramolecular gel can be reversible upon the heating and cooling process. In addition, the self-assembly properties of supramolecular gel can also be triggered through multiple stimuli such as pH, light and chemical species like metal cations and hydrogen bond acceptor anions (Hooper *et al.*, 2016). Supramolecular gel with a high aspect ratio and high loading capacity is found to be useful for the absorption of toxic cationic, anionic dyes and heavy metal ions from contaminated water (Christoff-tempesta *et al.*, 2018).

Removal of toxic metals, anions and organic dyes from wastewater requires remediation prior disposal to water or lands. Organic dyes in particular have now appears in thousands of different formulations which make them stable and hard to biodegradable (Han *et al.*, 2019). Various methods such as biological treatment, the use of dispersants, solidifiers, sorbents and skimmers have been developed over the years for wastewater treatments. However, all the methods described have their own limitations (Chetia *et al.*, 2020). Gel-based adsorption technique is one to be looking forward to in environmental remediation (De & Mondal, 2018).

Sengupta and co-workers (2014) have proposed an adsorption technique with the aid of supramolecular gels. The gels consist of larger surface areas and porous nature as well as the synthesized ligand which comprised of hydrophilic and hydrophobic group capable to provide the interaction with organic dyes. In dye absorption experiment, it was shown that this gel

can absorbed up to 94% of methyl orange dye. In other work, Baddi and co-workers (2016) have reported supramolecular gel consists of amide and urea with anion tunable properties. The addition of anions has disintegrated the gels possibly due to the disruption of hydrogen bonding networks in the gel.

Thiourea compounds, for examples a series of *N*-benzoyl thiourea derivatives have been shown to possess gelation properties due to the presence of N-H as hydrogen bond donor and C=O and C=S as hydrogen bond acceptors (Staicu *et al.*, 2018). In addition, *p*-nitrobenzene thiourea derivatives also formed stable organogel resulted from hydrogen bond interactions and Van der Waals forces (Cao *et al.*, 2018). Inspired by the availability of hydrogen bond donor unit in thiourea compounds, herein, we sought to study the gelation properties of bisthiourea compound that were synthesized from the reaction of 3 amino acids (glycine, alanine, phenylalanine) with two acid chlorides namely isophthaloyl dichloride (**3.1**-**3.3**) and terephthaloyl dichloride (**3.4**-**3.6**). Amino acid side chains are added to the bisthiourea derivatives purposely to increase more hydrogen bonding sites that would aid the formation of supramolecular gel as seen in the work published by Hooper and co-workers (Hooper *et al.*, 2016). In this study, we also reported the effect of metal cations such as Co^{2+}, Cu^{2+}, Ni^{2+}, Pb^{2+} and anions such as Cl^{-}, AcO^{-}, F^{-} to the gel network and the ability of the gel to absorb organic dyes such as bromocresol green, Eriochrome black-T and xylenol orange.

MATERIALS AND METHODS

All chemical purchased is of reagent grade and used without purification. The characterisation of ligand and metal complexes was performed via CHN analyses, FTIR, ^{1}H NMR spectroscopy and ^{13}C NMR spectroscopy. By using DMSO-d_6 solution as a solvent, the ^{1}H NMR and ^{13}C NMR spectra were recorded using a JEOL 500 MHz FT-NMR spectrophotometer at FSTS, UNIMAS. The CHNS analyses were recorded with FlashEA 1112 Series CHNS elemental analyzer at FSTS, UNIMAS. Infrared spectra were recorded using Elmer Spectrum GX Fourier-Transform Spectrometer (4000-370 cm^{-1}) as KBr disc. The characterisation of metal complexes was performed using CHNS analyses and FTIR spectroscopy. The morphology of the gels was examined using scanning electron microscopy (SEM) on a Nova NanoSEM 230 (FEI) Scanning Electron Microscope. The percentage of the organic dye absorption by the gel was measured using Ultraviolet-visible (UV-vis) spectroscopy model Perkin Elmer/Lambda.

Synthesis of Bisthiourea Compounds

Isophthaloyl dichloride or terephthaloyl dichloride (0.507 g, 2.5 mmol) and potassium thiocyanate (0.480 g, 5.0 mmol) were added into a round bottom flask containing 120 mL of acetone. The solution mixture was stirred for one hour at room temperature. The white precipitate (KCl) formed from the reaction was filtered out and removed. Amino acids (glycine 0.375 g, 5.0 mmol; alanine 0.445 g, 5.0 mmol; phenylalanine 0.826 g, 5.0 mmol) were added as rapidly as possible into the filtrate and the resulting mixture was stirred and heated for 18 hours (70 ^{o}C-80 ^{o}C) under reflux condition. The mixture was allowed to cool to room temperature and the resulting solid product was filtered out. The filtrate was added into a beaker and allowed to dry out at room temperature. The resulting precipitate was washed with distilled water for several times and recrystallized with ethanol to give pure product. The structure of the synthesized compounds was confirmed using CHNS elemental analysis, FT-IR and ^{1}H and ^{13}C NMR spectroscopy.

Compound **3.1**. Yield 0.863 g, 86.65%. Yellowish solid. Analytical Calculated for $C_{14}H_{14}N_4O_6S_2$ (398.41 g/mol): C 42.20; H 3.54; N 14.06; S 16.10. Found: C 41.73; H 3.84; N 13.45; S 15.67. ^{1}H NMR (DMSO-d_6, 500 MHz), δ (ppm): 4.36 (4H, t, *J* 4.5), 7.69 (1H, t, *J* 8), 8.14 (2H, t, *J* 4.5), 8.49 (1H, d, *J* 7.5) 11.09 (2H, d, *J* 5.25) 11.47 (2H, s). ^{13}C NMR (DMSO-d_6, 500 MHz), δ (ppm): 47.37 (CH_2), 129.57, 131.78, 132.42, 133.58 (C aromatic), 167.60 (C=O), 170.19 (COOH), 180.98 (C=S). IR (ν): *ν*(N-H) amide 3213 cm^{-1}, *ν*(C=O) carboxylic 1714 cm^{-1}, *ν*(C=O) amide 1666 cm^{-1}, *ν*(C=C) aromatic 1506 cm^{-1}, *ν*(C=S) 1210 cm^{-1}, *ν*(C-N) 1169 cm^{-1}.

Compound **3.2**. Yield 0.866 g, 81.24%. Pale yellowish solid. Analytical Calculated for $C_{16}H_{18}N_4O_6S_2$ (426.47 g/mol): C 45.06; H 4.25; N 13.14; S 15.04. Found: C 45.39; H 3.87; N 12.84; S 15.63. ^{1}H NMR (DMSO-d_6, 500 MHz), δ (ppm): 1.51 (6H, d, *J* 6.5), 4.85 (2H, t, *J* 7.25), 7.69 (1H, t, *J* 7.75), 8.14 (2H, d, *J* 8), 8.50 (1H, s), 11.26 (2H, d, *J* 7.5), 11.47 (2H, s). ^{13}C NMR (DMSO-d_6, 500 MHz), δ (ppm): 17.54, 17.80

(CH_3), 53.18, 54.30 (CH), 129.30, 129.51, 132.32, 133.47, 133.72 (C aromatic), 167.91 (C=O), 173.35 (COOH), 180.03 (C=S). IR (ν): *ν*(N-H) amide 3222 cm^{-1}, *ν*(C=O) carboxylic 1725 cm^{-1}, *ν*(C=O) amide 1690 cm^{-1}, *ν*(C=C) aromatic 1502 cm^{-1}, *ν*(C=S) 1210 cm^{-1}, *ν*(C-N) 1172 cm^{-1}.

Compound **3.3**. Yield 1.093 g, 75.54%. Yellowish solid. Analytical Calculated for $C_{28}H_{26}N_4O_6S_2$ (578.66 g/mol): C 58.12; H 4.53; N 9.68; S 11.08. Found: C 57.65; H 4.09; N 10.01; S 11.36. ^{1}H NMR (DMSO-d_6, 500 MHz), δ (ppm): 3.21 (2H, m, *J* 6.5), 3.37 (2H, t, *J* 6.75), 5.16 (2H, m, *J* 5.5), 7.26 (10H, m, *J* 7), 7.66 (1H, d, *J* 8), 8.10 (2H, d, *J* 7.5), 8.49 (1H, s), 11.18 (2H, d, *J* 7.5), 11.53 (2H, s). ^{13}C NMR (DMSO-d_6, 500 MHz), δ (ppm): 36.65 (CH_2), 58.60, 58.87 (CH), 126.93, 127.87, 128.43, 129.26, 129.36, 130.19, 132.15, 136.68 (C aromatic), 167.85 (C=O), 171.80 (COOH), 180.53 (C=S). IR (ν): *ν*(N-H) amide 3222 cm^{-1}, *ν*(C=O) carboxylic 1716 cm^{-1}, *ν*(C=O) amide 1689 cm^{-1}, *ν*(C=C) aromatic 1506 cm^{-1}, *ν*(C=S) 1204 cm^{-1}, *ν*(C-N) 1167 cm^{-1}.

Compound **3.4**. Yield 0.866 g, 86.95%. Yellowish solid. Analytical Calculated for $C_{14}H_{14}N_4O_6S_2$ (398.41 g/mol): C 42.20; H 3.54; N 14.06; S 16.10. Found: C 41.64; H 3.07; N 13.56; S 16.41. ^{1}H NMR (DMSO-d_6, 500 MHz), δ (ppm): 2.67 (1H, m, *J* 6.5), 3.03 (1H, m, *J* 10), 3.78 (4H, d, *J* 13), 5.54 (1H, m, *J* 5), 6.23 (2H, m, *J* 6), 7.42 (2H, m, *J* 8), 7.51 (2H, d, *J* 6.5). ^{13}C NMR (DMSO-d_6, 500 MHz), δ (ppm): 45.20 (CH_2), 126.74, 127.15, 128.69, 129.26 (C aromatic), 162.23 (C=O), 164.69, 165.87 (COOH), 188.11 (C=S). IR (ν): *ν*(N-H) amide 3223 cm^{-1}, *ν*(C=O) carboxylic 1716 cm^{-1}, *ν*(C=O) amide 1666 cm^{-1}, *ν*(C=C) aromatic 1518 cm^{-1}, *ν*(C=S) 1249 cm^{-1}, *ν*(C-N) 1172 cm^{-1}.

Compound **3.5**. Yield 0.808 g, 75.80%. Yellowish solid. Analytical Calculated for $C_{16}H_{18}N_4O_6S_2$ (426.47 g/mol): C 45.06; H 4.25; N 13.14; S 15.04. Found: C 45.42; H 3.77; N 12.88; S 14.64. ^{1}H NMR (DMSO-d_6, 500 MHz), δ (ppm): 1.31 (6H, t, *J* 6.75), 4.53 (2H, m, *J* 7.5), 7.98 (5H, s), 8.04 (1H, t, *J* 10.25), 12.11 (2H, s). ^{13}C NMR (DMSO-d_6, 500 MHz), δ (ppm): 13.89 (CH_3), 67.81 (CH), 128.88, 129.78, 134.77, 137.02 (C aromatic), 164.88 (C=O), 166.99 (COOH), 189.74 (C=S). IR (ν): *ν*(N-H) amide 3172cm^{-1}, *ν*(C=O) carboxylic 1715 cm^{-1}, *ν*(C=O) amide 1665 cm^{-1}, *ν*(C=C) aromatic 1501 cm^{-1}, *ν*(C=S) 1255 cm^{-1}, *ν*(C-N) 1152 cm^{-1}.

Compound **3.6**. Yield 1.130 g, 78.09%. Yellowish solid. Analytical Calculated for $C_{28}H_{26}N_4O_6S_2$ (578.66 g/mol): C 58.12; H 4.53; N 9.68; S 11.08. Found: C 57.63; H 4.06; N 9.83; S 11.45. ^{1}H NMR (DMSO-d_6, 500 MHz), δ (ppm): 3.20 (2H, m, *J* 6), 3.36 (2H, t, *J* 7), 5.14 (2H, m, *J* 6), 7.26 (4H, m, *J* 7.5), 7.94 (2H, d, *J* 13), 8.01 (10H, m, *J* 10.5), 11.15 (2H, d, *J* 7.5), 11.71 (2H, s). ^{13}C NMR (DMSO-d_6, 500 MHz), δ (ppm): 36.54 (CH_2), 59.25 (CH), 127.40, 127.92, 128.91, 129.64, 129.77, 129.97, 136.26, 136.75 (C aromatic), 168.14 (C=O), 171.86 (COOH), 180.56 (C=S). IR (ν): *ν*(N-H) amide 3026 cm^{-1}, *ν*(C=O) carboxylic 1717 cm^{-1}, *ν*(C=O) amide 1667 cm^{-1}, *ν*(C=C) aromatic 1499 cm^{-1}, *ν*(C=S) 1256 cm^{-1}, *ν*(C-N) 1159 cm^{-1}.

General Procedure for the Synthesis of Metal Complexes

Bisthiourea ligand (0.30 mmol) was dissolved in 30 mL of ethanol in round bottom flask with addition of potassium hydroxide (0.034 g, 0.60 mmol). The mixture was stirred for 30 minutes. Next, immediately added the metal (cobalt(II) chloride-6-hydrate 0.072 g, 0.30 mmol; copper(II) chloride-2-hydrate 0.052 g, 0.30 mmol; nickel chloride-6-hydrate 0.072 g, 0.30 mmol; lead(II) nitrate 0.10 g, 0.30 mmol) into the resulting mixture based on ratio of 1:1 (ligand: metal). The mixture was stirred again for two hours at room temperature. The solid formed from the mixture was filtered, washed and dried to afford the product. The solid formed was washed with distilled water for several times and recrystallized with methanol to give pure product. The structure of the synthesized compounds was confirmed using CHNS elemental analysis and FTIR spectroscopy.

Compound **3.1a**. Yield 0.110 g, 74.83%. Purple solid. Analytical Calculated for $C_{28}H_{32}N_8Co_2O_{16}S_4$ (982.73 g/mol): C 34.22; H 3.28; N 11.99; S 13.05. Found: C 34.53; H 3.07; N 11.75; S 13.26. IR (*ν*): *ν*(N-H) amide 3222 cm^{-1}, *ν*(C=O) amide 1668 cm^{-1}, *ν*(C=C) aromatic 1502 cm^{-1}, *ν*(C=S) 1227 cm^{-1}, *ν*(C-N) 1166 cm^{-1}.

Compound **3.1b**. Yield 0.104 g, 75.36%. Green solid. Analytical Calculated for $C_{28}H_{24}N_8Cu_2O_{12}S_4$ (919.89 g/mol): C 36.56; H 2.63; N 12.18; S 13.94. Found: C 36.38; H 2.38;

N 12.25; S 14.01. IR (*v*): *v*(N-H) amide 3252 cm^{-1}, *v*(C=O) amide 1674 cm^{-1}, *v*(C=C) aromatic 1506 cm^{-1}, *v*(C=S) 1228 cm^{-1}, *v*(C-N) 1178 cm^{-1}.

Compound **3.1c**. Yield 0.106 g, 77.37%. Orange solid. Analytical Calculated for $C_{28}H_{24}N_8Ni_2O_{12}S_4$ (910.19 g/mol): C 36.95; H 2.66; N 12.31; S 14.09. Found: C 37.08; H 2.83; N 12.54; S 13.91. IR (*v*): *v*(N-H) amide 3216 cm^{-1}, *v*(C=O) amide 1667 cm^{-1}, *v*(C=C) aromatic 1501 cm^{-1}, *v*(C=S) 1226 cm^{-1}, *v*(C-N) 1166 cm^{-1}.

Compound **3.1d**. Yield 0.139 g, 72.40%. White solid. Analytical Calculated for $C_{28}H_{32}N_8Pb_2O_{16}S_4$ (1279.26 g/mol): C 26.29; H 2.52; N 8.76; S 10.03. Found: C 25.98; H 2.38; N 8.93; S 10.19. IR (*v*): *v*(N-H) amide 3228 cm^{-1}, *v*(C=O) amide 1671 cm^{-1}, *v*(C=C) aromatic 1506 cm^{-1}, *v*(C=S) 1229 cm^{-1}, *v*(C-N) 1174 cm^{-1}.

Compound **3.2a**. Yield 0.112 g, 71.79%. Purple solid. Analytical Calculated for $C_{32}H_{40}N_8Co_2O_{16}S_4$ (1038.83 g/mol): C 37.00; H 3.88; N 10.79; S 12.35. Found: C 36.81; H 4.16; N 10.88; S 11.96. IR (*v*): *v*(N-H) amide 3211 cm^{-1}, *v*(C=O) amide 1671 cm^{-1}, *v*(C=C) aromatic 1485 cm^{-1}, *v*(C=S) 1227 cm^{-1}, *v*(C-N) 1139 cm^{-1}.

Compound **3.2b**. Yield 0.102 g, 69.86%. Green solid. Analytical Calculated for $C_{32}H_{32}N_8Cu_2O_{12}S_4$ (976.00 g/mol): C 39.38; H 3.30; N 11.48; S 13.14. Found: C 39.80; H 2.98; N 11.09; S 13.23. IR (*v*): *v*(N-H) amide 3255 cm^{-1}, *v*(C=O) amide 1665 cm^{-1}, *v*(C=C) aromatic 1460 cm^{-1}, *v*(C=S) 1235 cm^{-1}, *v*(C-N) 1153 cm^{-1}.

Compound **3.2c**. Yield 0.108 g, 74.48%. Green solid. Analytical Calculated for $C_{32}H_{32}N_8Ni_2O_{12}S_4$ (966.29 g/mol): C 39.77; H 3.34; N 11.60; S 13.27. Found: C 40.02; H 3.21; N 11.54; S 13.18. IR (*v*): *v*(N-H) amide 3198 cm^{-1}, *v*(C=O) amide 1672 cm^{-1}, *v*(C=C) aromatic 1503 cm^{-1}, *v*(C=S) 1233 cm^{-1}, *v*(C-N) 1138 cm^{-1}.

Compound **3.2d**. Yield 0.146 g, 73.00%. White solid. Analytical Calculated for $C_{32}H_{40}N_8Pb_2O_{16}S_4$ (1335.37 g/mol): C 28.78; H 3.02; N 8.39; S 9.60. Found: C 28.44; H 3.09; N 8.52; S 9.48. IR (*v*): *v*(N-H) amide 3222 cm^{-1}, *v*(C=O) amide 1675 cm^{-1}, *v*(C=C) aromatic 1512 cm^{-1}, *v*(C=S) 1242 cm^{-1}, *v*(C-N) 1177 cm^{-1}.

Compound **3.3a**. Yield 0.160 g, 79.60%. Purple solid. Analytical Calculated for $C_{56}H_{56}N_8Co_2O_{16}S_4$ (1343.22 g/mol): C 50.07; H 4.20; N 8.34; S 9.55. Found: C 49.86; H 4.24; N 8.25; S 9.50. IR (*v*): *v*(N-H) amide 3226 cm^{-1}, *v*(C=O) amide 1669 cm^{-1}, *v*(C=C) aromatic 1501 cm^{-1}, *v*(C=S) 1234 cm^{-1}, *v*(C-N) 1166 cm^{-1}.

Compound **3.3b**. Yield 0.137 g, 71.35%. Green solid. Analytical Calculated for $C_{56}H_{48}N_8Cu_2O_{12}S_4$ (1280.38 g/mol): C 52.53; H 3.78; N 8.75; S 10.02. Found: C 52.38; H 4.02; N 8.78; S 10.21. IR (*v*): *v*(N-H) amide 3261 cm^{-1}, *v*(C=O) amide 1681 cm^{-1}, *v*(C=C) aromatic 1506 cm^{-1}, *v*(C=S) 1231 cm^{-1}, *v*(C-N) 1171 cm^{-1}.

Compound **3.3c**. Yield 0.149 g, 78.01%. Green solid. Analytical Calculated for $C_{56}H_{48}N_8Ni_2O_{12}S_4$ (1270.68 g/mol): C 52.93; H 3.81; N 8.82; S 10.09. Found: C 52.85; H 4.03; N 8.62; S 10.12. IR (*v*): *v*(N-H) amide 3228 cm^{-1}, *v*(C=O) amide 1672 cm^{-1}, *v*(C=C) aromatic 1499 cm^{-1}, *v*(C=S) 1234 cm^{-1}, *v*(C-N) 1164 cm^{-1}.

Compound **3.3d**. Yield 0.176 g, 71.54%. White solid. Analytical Calculated for $C_{56}H_{56}N_8Pb_2O_{16}S_4$ (1639.75 g/mol): C 41.02; H 3.44; N 6.83; S 7.82. Found: C 40.88; H 3.45; N 6.62; S 7.87. IR (*v*): *v*(N-H) amide 3186 cm^{-1}, *v*(C=O) amide 1675 cm^{-1}, *v*(C=C) aromatic 1512 cm^{-1}, *v*(C=S) 1205 cm^{-1}, *v*(C-N) 1152 cm^{-1}.

Compound **3.4a**. Yield 0.117 g, 79.59%. Purple solid. Analytical Calculated for $C_{28}H_{32}N_8Co_2O_{16}S_4$ (982.73 g/mol): C 34.22; H 3.28; N 11.40; S 13.05. Found: C 34.53; H 3.27; N 11.54; S 12.87. IR (*v*): *v*(N-H) amide 3216 cm^{-1}, *v*(C=O) amide 1666 cm^{-1}, *v*(C=C) aromatic 1512 cm^{-1}, *v*(C=S) 1243 cm^{-1}, *v*(C-N) 1163 cm^{-1}.

Compound **3.4b**. Yield 0.099 g, 71.74%. Green solid. Analytical Calculated for $C_{28}H_{24}N_8Cu_2O_{12}S_4$ (919.89 g/mol): C 36.56; H 2.63; N 12.18; S 13.94. Found: C 36.73; H 2.96; N 12.23; S 13.79. IR (*v*): *v*(N-H) amide 3195 cm^{-1}, *v*(C=O) amide 1668 cm^{-1}, *v*(C=C) aromatic 1512 cm^{-1}, *v*(C=S) 1226 cm^{-1}, *v*(C-N) 1172 cm^{-1}.

Compound **3.4c**. Yield 0.103 g, 75.18%. Orange solid. Analytical Calculated for $C_{28}H_{24}N_8Ni_2O_{12}S_4$ (910.19 g/mol): C 36.95; H 2.66; N 12.31; S 14.09. Found: C 36.79; H 2.63; N 12.25; S 14.17. IR (*v*): *v*(N-H) amide 3201 cm^{-1}, *v*(C=O) amide 1666 cm^{-1}, *v*(C=C) aromatic 1510 cm^{-1}, *v*(C=S) 1277 cm^{-1}, *v*(C-N) 1169 cm^{-1}.

Compound **3.4d**. Yield 0.145 g, 75.52%. White solid. Analytical Calculated for

$C_{28}H_{32}N_8Pb_2O_{16}S_4$ (1279.26 g/mol): C 26.29; H 2.52; N 8.76; S 10.03. Found: C 25.98; H 2.23; N 8.62; S 10.12. IR (*v*): *v*(N-H) amide 3225 cm^{-1}, *v*(C=O) amide 1680 cm^{-1}, *v*(C=C) aromatic 1515 cm^{-1}, *v*(C=S) 1282 cm^{-1}, *v*(C-N) 1176 cm^{-1}.

Compound **3.5a**. Yield 0.125 g, 80.13%. Purple solid. Analytical Calculated for $C_{32}H_{40}N_8Co_2O_{16}S_4$ (1038.83 g/mol): C 37.00; H 3.88; N 10.79; S 12.35. Found: C 36.92; H 4.12; N 10.71; S 12.40. IR (*v*): *v*(N-H) amide 3203 cm^{-1}, *v*(C=O) amide 1666 cm^{-1}, *v*(C=C) aromatic 1489 cm^{-1}, *v*(C=S) 1255 cm^{-1}, *v*(C-N) 1151 cm^{-1}.

Compound **3.5b**. Yield 0.114 g, 78.08%. Green solid. Analytical Calculated for $C_{32}H_{32}N_8Cu_2O_{12}S_4$ (976.00 g/mol): C 39.38; H 3.30; N 11.48; S 13.14. Found: C 39.57; H 3.59; N 11.23; S 13.21. IR (*v*): *v*(N-H) amide 3166 cm^{-1}, *v*(C=O) amide 1668 cm^{-1}, *v*(C=C) aromatic 1513 cm^{-1}, *v*(C=S) 1254 cm^{-1}, *v*(C-N) 1170 cm^{-1}.

Compound **3.5c**. Yield 0.101 g, 69.66%. Green solid. Analytical Calculated for $C_{32}H_{32}N_8Ni_2O_{12}S_4$ (966.29 g/mol): C 39.77; H 3.34; N 11.60; S 13.27. Found: C 39.47; H 3.52; N 11.64; S 13.32. IR (*v*): *v*(N-H) amide 3224 cm^{-1}, *v*(C=O) amide 1665 cm^{-1}, *v*(C=C) aromatic 1508 cm^{-1}, *v*(C=S) 1260 cm^{-1}, *v*(C-N) 1157 cm^{-1}.

Compound **3.5d**. Yield 0.155 g, 77.50%. White solid. Analytical Calculated for $C_{32}H_{40}N_8Pb_2O_{16}S_4$ (1335.37 g/mol): C 28.78; H 3.02; N 8.39; S 9.60. Found: C 28.64; H 2.92; N 8.23; S 9.67. IR (*v*): *v*(N-H) amide 3224 cm^{-1}, *v*(C=O) amide 1671 cm^{-1}, *v*(C=C) aromatic 1510 cm^{-1}, *v*(C=S) 1261 cm^{-1}, *v*(C-N) 1171 cm^{-1}.

Compound **3.6a**. Yield 0.148 g, 73.63%. Purple solid. Analytical Calculated for $C_{56}H_{56}N_8Co_2O_{16}S_4$ (1343.22 g/mol): C 50.07; H 4.20; N 8.34; S 9.55. Found: C 50.24; H 4.32; N 8.26; S 9.57. IR (*v*): *v*(N-H) amide 3229 cm^{-1}, *v*(C=O) amide 1674 cm^{-1}, *v*(C=C) aromatic 1501 cm^{-1}, *v*(C=S) 1259 cm^{-1}, *v*(C-N) 1161 cm^{-1}.

Compound **3.6b**. Yield 0.144 g, 75.00%. Green solid. Analytical Calculated for $C_{56}H_{48}N_8Cu_2O_{12}S_4$ (1280.38 g/mol): C 52.53; H 3.78; N 8.75; S 10.02. Found: C 52.58; H 4.01; N 8.67; S 10.10. IR (*v*): *v*(N-H) amide 3216 cm^{-1}, *v*(C=O) amide 1673 cm^{-1}, *v*(C=C) aromatic 1515 cm^{-1}, *v*(C=S) 1255 cm^{-1}, *v*(C-N) 1168 cm^{-1}.

Compound **3.6c**. Yield 0.132 g, 69.11%. Green solid. Analytical Calculated for $C_{56}H_{48}N_8Ni_2O_{12}S_4$ (1270.68 g/mol): C 52.93; H 3.81; N 8.82; S 10.09. Found: C 52.67; H 3.87; N 8.91; S 10.01. IR (*v*): *v*(N-H) amide 3228 cm^{-1}, *v*(C=O) amide 1672 cm^{-1}, *v*(C=C) aromatic 1491 cm^{-1}, *v*(C=S) 1260 cm^{-1}, *v*(C-N) 1161 cm^{-1}.

Compound **3.6d**. Yield 0.183 g, 74.39%. White solid. Analytical Calculated for $C_{56}H_{56}N_8Pb_2O_{16}S_4$ (1639.75 g/mol): C 41.02; H 3.44; N 6.83; S 7.82. Found: C 41.05; H 3.41; N 6.75; S 7.93. IR (*v*): *v*(N-H) amide 3230 cm^{-1}, *v*(C=O) amide 1672 cm^{-1}, *v*(C=C) aromatic 1503 cm^{-1}, *v*(C=S) 1263 cm^{-1}, *v*(C-N) 1160 cm^{-1}.

Gelation Studies of Bisthiourea Compounds

The bisthiourea derivatives synthesized were tested for their gelation properties. Typically, 10 mg of ligand and 0.5 mL of the appropriate solvent were placed in 2 mL sample vials (taken to be 2 wt%) and gently heated for three minutes. Then, the mixtures were immediately sonicated for about 30s and allowed to cool to room temperature. For DCM solvent, water was added in portion by 10 µL each to the mixture and the heating-cooling process was continued until it reaches the gelation state. The formation of precipitates, gels or crystals were observed through its gravitational flow. A sample is defined as a gel if there is no gravitational flow upon turning the vial upside down. The critical gelation concentration (CGC), defined as the minimum concentration of gelator necessary for gelation was determined experimentally. The morphology of the gel was observed using scanning electron microscope (SEM).

Cation Addition of Bisthiourea Compounds

The reaction was taken place in 2 mL sample vials with addition of 10 mg of ligand and 0.5 mL solvent (taken to be 2 wt%). Subsequently, 10 µL of potassium hydroxide and metallic salts were added into the vials. The mixtures were gently heated and immediately sonicated for 30s in which the solubility of the compound was recorded. Samples were allowed to cool to room temperature and the formation of precipitates, gels or crystals were observed through its gravitational flow upon turning vial upside-down. The morphology of the gel was observed

using scanning electron microscope (SEM).

Anion Addition of Bisthiourea Compounds

For the naked-eye sensing test of gelation with different anions, a solution of the anions (F^-, Cl^-, AcO^-) as tetrabutylammonium salts with appropriate ratio were added to the gel of the respective solvents. The sample vials were inverted after 24 hours to determine the gel–sol transition.

Organic Dyes Removal

For organic dyes absorption tests, 0.5 mL of the dye solution (bromocresol green, Eriochrome black-T and xylenol orange) were introduced to the 50:3 dichloromethane:water mixture gel. The stock solutions of the respective dyes were prepared by dissolving 1, 2, 3 and 4 mg of dye in 100 mL of water at room temperature. The changes in the absorption bands were recorded in timely manner (1h, 2h, 3h, 6h, 12h and 24 h) using UV-Vis spectroscopy. The absorbance of supernatant liquid at 400 nm (bromocresol green) and 517 nm (Eriochrome black-T) was used to estimate the concentration of the remaining dyes. The morphology of the gels after the addition of the dyes were observed using scanning electron microscope (SEM) (Jeol Ltd., Japan).

RESULTS AND DISCUSSION

Synthesis of Bisthiourea Compounds

The formation of bisthiourea compounds **3.1**-**3.6** were accomplished by reacting the isothiocyanate intermediates with respective amino acids (glycine, alanine and phenylalanine) as shown in Scheme 1. The first step produced isophthaloyl and terephthaloyl isothiocyanate intermediates, which were then reacted with chosen amino acids to furnish compounds **3.1**, **3.2**, **3.3**, **3.4**, **3.5** and **3.6** with the overall yield of 86.65%, 81.24%, 75.54%, 86.95%, 75.80% and 78.09%, respectively. Elemental analysis data for the synthesized derivatives were found to be in good agreement with the theoretical values.

The Fourier Transform Infra-Red (FT-IR) spectra of compounds **3.1**-**3.6** shows all the basic functional group peaks (Figure 1). The broad peaks at 3400-3100 cm^{-1} indicate the OH and NH stretching peaks. The distinctive peaks at 1725-1714 cm^{-1} are attributed to *ν*(C=O) carboxylic while the peaks at 1690-1665 cm^{-1} indicated *ν*(C=O) amide. The peak observed at 1256-1204 cm^{-1} are attributed to *ν*(C=S) while peak observed at 1172-1152 cm^{-1} are of *ν*(C-N) functionality (Fakhar *et al.*, 2016) (Table 1).

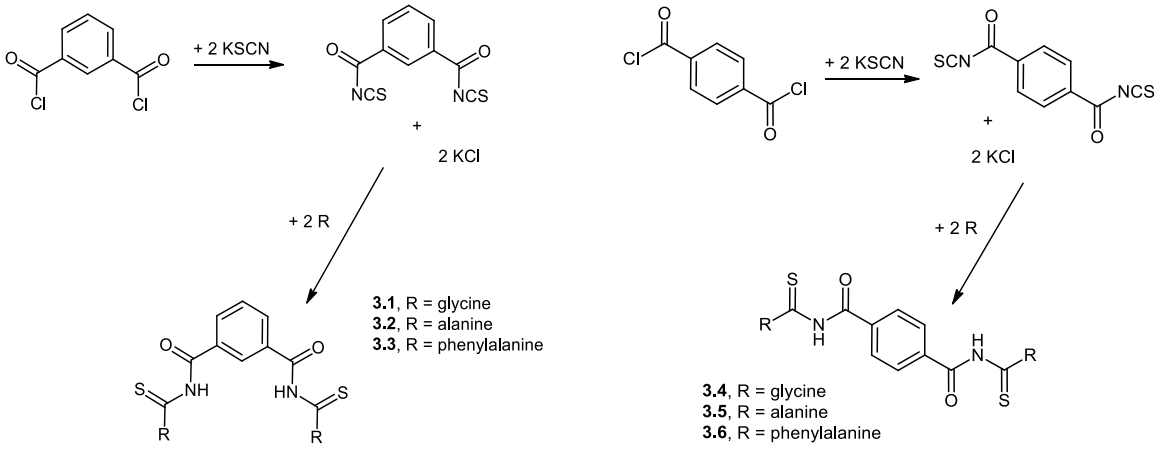

Scheme 1. Synthesis pathway of compounds **3.1**-**3.6**

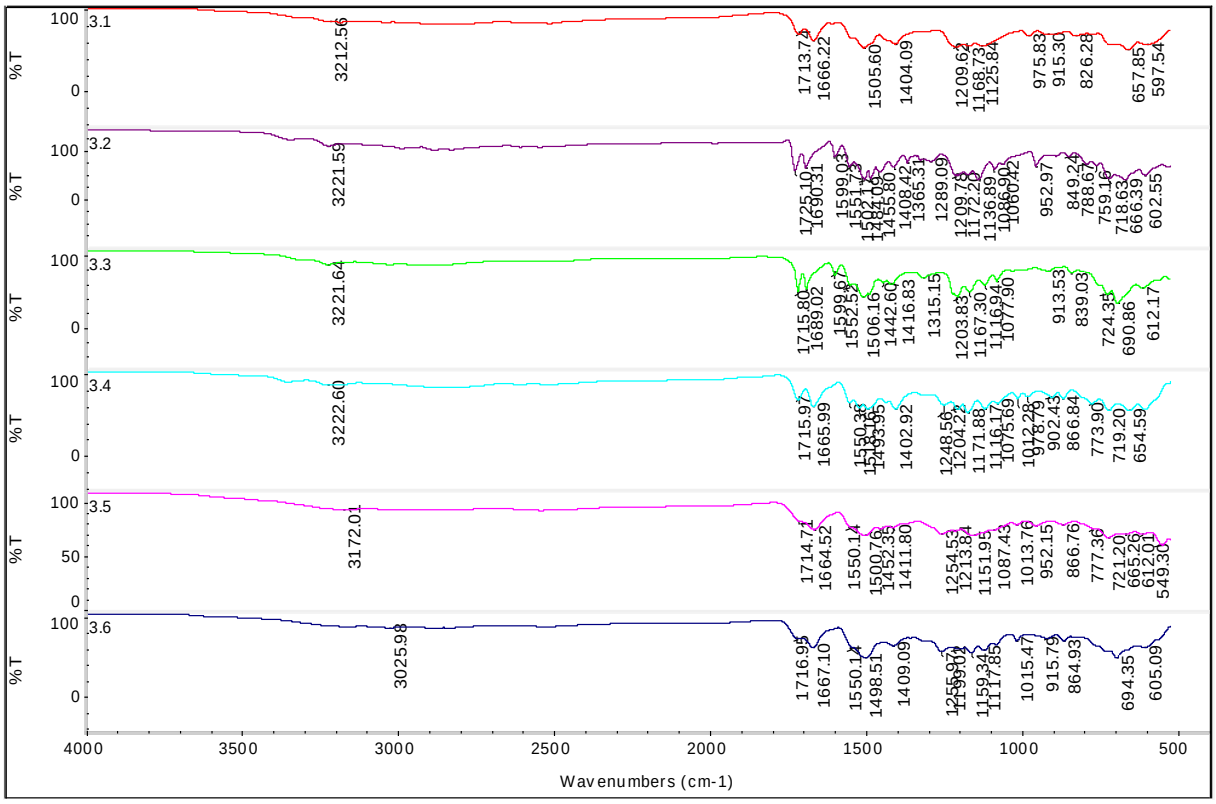

Figure 1. FTIR spectra of compounds **3.1**-**3.6**

Table 1. Important FTIR stretching vibration of compounds **3.1**-**3.6**

Compound	Wavelength (cm^{-1})			
	v(C=O) carboxylic	*v*(C=O) amide	*v*(C=S)	*v*(C-N)
3.1	1714	1666	1210	1169
3.2	1725	1690	1210	1172
3.3	1716	1689	1204	1167
3.4	1716	1666	1249	1152
3.5	1715	1665	1255	1152
3.6	1717	1667	1256	1159

Screening of Compounds for Gel Properties

The gelation behavior of **3.1**-**3.6** were examined in 17 solvents including polar solvents such as methanol, ethanol and propanol, non-polar solvents such as hexane, toluene and petroleum ether, and polar aprotic solvents such as ethyl acetate, acetone and acetonitrile (Hooper *et al.*, 2016). The vial was turned upside down to observe the formation of a gel. Table 2 summarizes the screening of those six compounds in a range of common laboratory solvents.

Table 2. Gelation tests for compounds **3.1**, **3.2**, **3.3**, **3.4**, **3.5** and **3.6**

Solvent	Observation (Compound)					
	3.1	**3.2**	**3.3**	**3.4**	**3.5**	**3.6**
Methanol	Ss	S	S	Ss	S	S
Ethanol	Ss	S	S	Ss	S	S
Propanol	Ss	S	S	Ss	S	S
Hexane	I	I	I	I	I	I
Dimethyl sulfoxide (DMSO)	S	S	S	S	S	S
Acetonitrile	I	Ss	I	I	I	I
Distilled water	I	I	I	I	I	I
Tetrahydrofuran (THF)	S	S	S	Ss	S	S
Toluene	I	I	I	I	I	I
Ethyl acetate	I	I	I	I	I	I
Dichloromethane (DCM)	I	I	I	I	G	I
Chloroform	I	I	I	I	I	Ss
Acetone	Ss	Ss	S	Ss	Ss	S
Diethyl ether	I	I	I	I	I	I
Cyclohexanol	S	S	S	Ss	S	S
Petroleum ether	I	I	I	I	I	I
Nitromethane	I	I	I	I	I	I

*G=gel, S=soluble, I=insoluble, Ss=suspension

The synthesized compounds were found to be soluble in polar solvent such as methanol, ethanol and propanol and in polar aprotic solvent such as acetone and DMSO possibly due to the polarity of the solvent. However, the synthesized compounds did not form any gel in these solvents possibly because the hydrogen bonds in the solvents competes with the hydrogen bonds in compounds which prevent the formation of hydrogen bond networks that are responsible for the gelation (Liu *et al.*, 2016). Interestingly, only compound **3.5** formed opaque gel in polar aprotic solvent, dichloromethane at room temperature. This is possibly because dichloromethane is capable of forming balanced gelator-gelator and solvent-gelator interactions (Liu *et al.*, 2016). However, the addition of 30 ml of distilled water in the dichloromethane gel resulted a stronger gel which leads to a plateau stability (Tatikonda *et al.*, 2016). The addition of water which involving one hydrogen atom positioned between the two oxygen atoms could possibly enhance the strong intermolecular hydrogen bonding between the gelator molecules as it attracted to other polar molecules and to ions (Panja & Ghosh, 2018). The critical gelation concentration of dichloromethane was observed at 2% w/v, 1% w/v and 0.5% w/v. Thus, it can be identified that the solvent is immobilize when the gelator concentration exceed a critical point (Bachl *et al.*, 2017).

Supramolecular gels were found to be responsive towards physical and chemical stimuli which can control and modulate the gel properties (Wezenberg *et al.*, 2016). Since 50:3 dichloromethane:water mixture able to form opaque gel, an experiment was further conducted to evaluate its thermoreversibility property. The transition of gel-sol was observed at 2% w/v upon sonication and heating due to mechanical disturbances. When the solution was cooled down, it reverted into gel phase due to the self-assembly of the molecules. It can be concluded that heating the gel would destroy the hydrogen bonding interaction between the molecules since the gel formation was induced from small molecules assembly through interactions of π-π

stacking, van der Waals forces interactions, hydrogen bonding or hydrophobic/solvophobic effect (Cheng *et al.*, 2018). Often, high temperature is needed to break the strong intermolecular forces between the molecules. Repeated heating and cooling showed similar transition behaviour as shown in Figure 2.

To obtain further insight into solvent effect on the self-assembly property of this gelator, scanning electron microscopy (SEM) was used to investigate the micro-scale structures of the gel formed in 50:3 dichloromethane:water mixture. As evidenced by SEM images shown in Figure 3, the gel revealed the formation of entangled cross-linked fibres which worked as the main microstructures to support the formation of organogel. The mean of entangled fibre is 0.16 µm with the maximum and the minimum width are 0.17 µm and 0.13 µm, respectively.

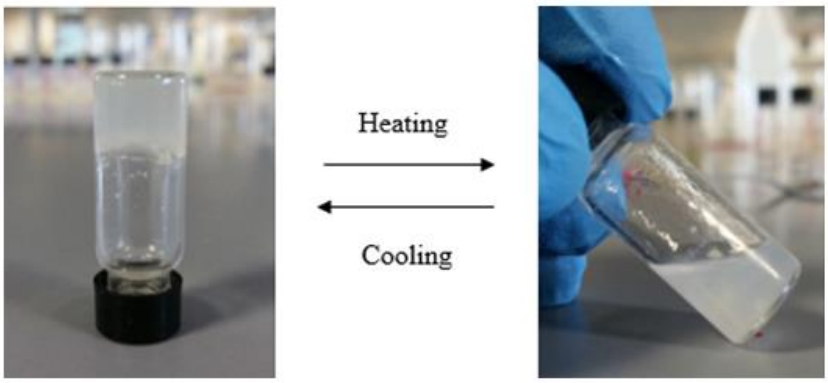

Figure 2. Thermoreversible gel of 50:3 dichloromethane:water mixture

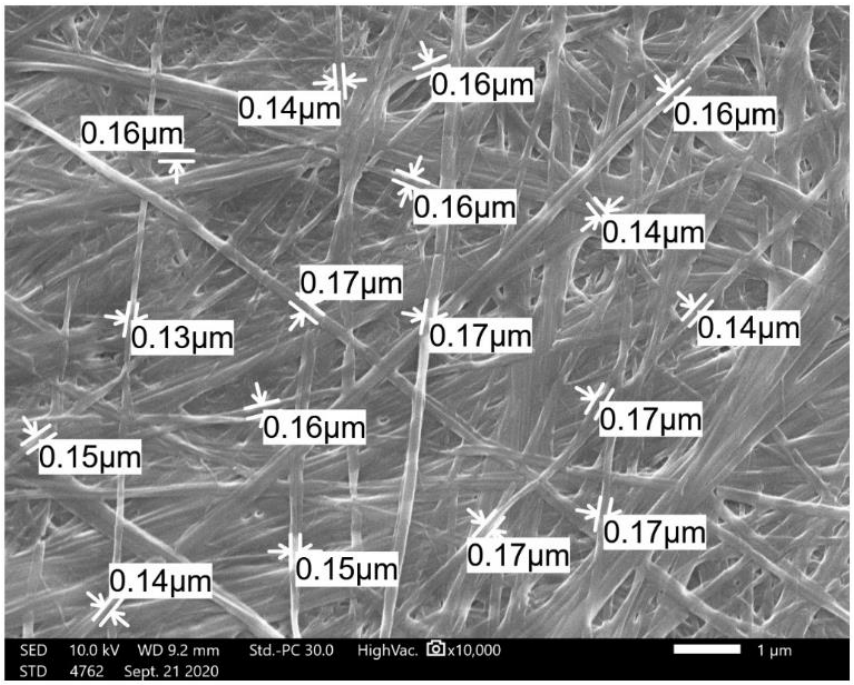

Figure 3. SEM images of 50:3 dichloromethane:water mixture gel

Complexation Reactions of Bisthiourea Compounds

To observe whether the bisthiourea compounds can be used to extract metal ions through the formation of metallogel, complexation reactions have been carried out between compound **3.1-3.6** with $CoCl_2{\cdot}6H_2O$ (**a**), $CuCl{\cdot}2H_2O$ (**b**), $NiCl_2{\cdot}6H_2O$ (**c**) and $Pb(NO_3)_2$ (**d**) as shown in Scheme 2. The gelation test was conducted in 17 different solvents. In each of the vials, equimolar potassium hydroxide was added to aid the deprotonation of the OH group of carboxylic acid moiety for the complexation reactions to occur.

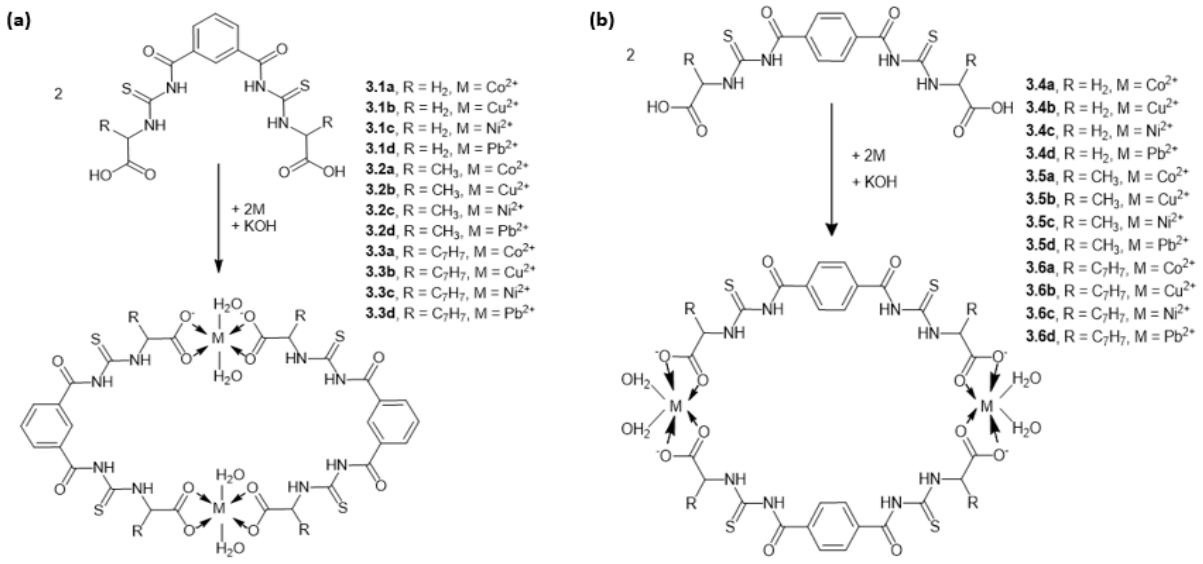

Scheme 2. Synthesis pathway of metal complexes (a) **3.1-3.3 (a-d)** and (b) **3.4-3.6 (a-d)**

The addition of the metal salts has caused colour changes to most of the ligand solutions indicating complexation reactions between the ligands (**3.1-3.6**) and the metal salts. However, none of the metals were able to form metallogels as anticipated. It is suggested that the addition of the metal salts which contain counter anions (Cl^- and NO_3^-) has possibly interrupted the hydrogen bond interaction between the thiourea molecules, thus the formation of metallogel was not observed. This observation is in agreement with the published work of Tatikonda and co-workers which shows that the presence of anion (Cl^-) leads to complete loss of gelation attitude (Tatikonda *et al.*, 2016). From another perspective, the presence of amide group in the structure could also form competitive hydrogen bonding with anion that inhibit the formation of a gel (Li *et al.*, 2019).

To confirm the formation of metal complexes, the precipitates obtained from the gelation tests have been subjected to characterization using elemental analysis and FTIR spectroscopy. Elemental analysis data for the synthesized metal complexes were found to be in close accordance with the theoretical values.

The Fourier Transform Infra-Red (FTIR) spectra (Figure 4) of complexes have been compared with their respective ligands. There is a broad band between 3400-3100 cm^{-1}, indicates OH stretch due to incorporation of water molecules towards the central metal atom. The shifting of *v*(C=O) carboxylic peaks at 1725-1714 cm^{-1} and the appearance of *v*(C=O) amide at 1681-1665 cm^{-1} proved that the metal atoms were coordinated to the carboxylate group as shown in Figures 4-9. The absorption frequencies at 1263-1226 cm^{-1} represented *v*(C=S) shows an increase in the wavenumber due to the reactions of ligands with metal ions (Table 3).

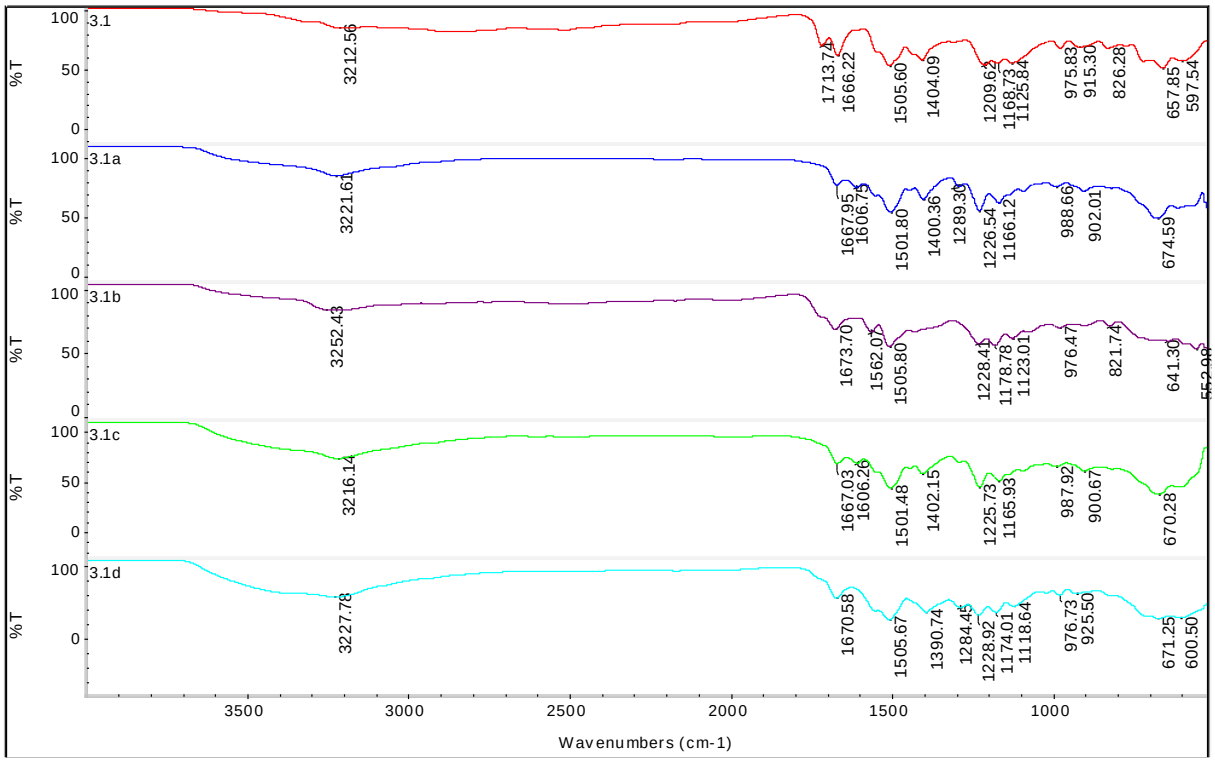

Figure 4. FTIR spectra of metal complexes of compound **3.1**

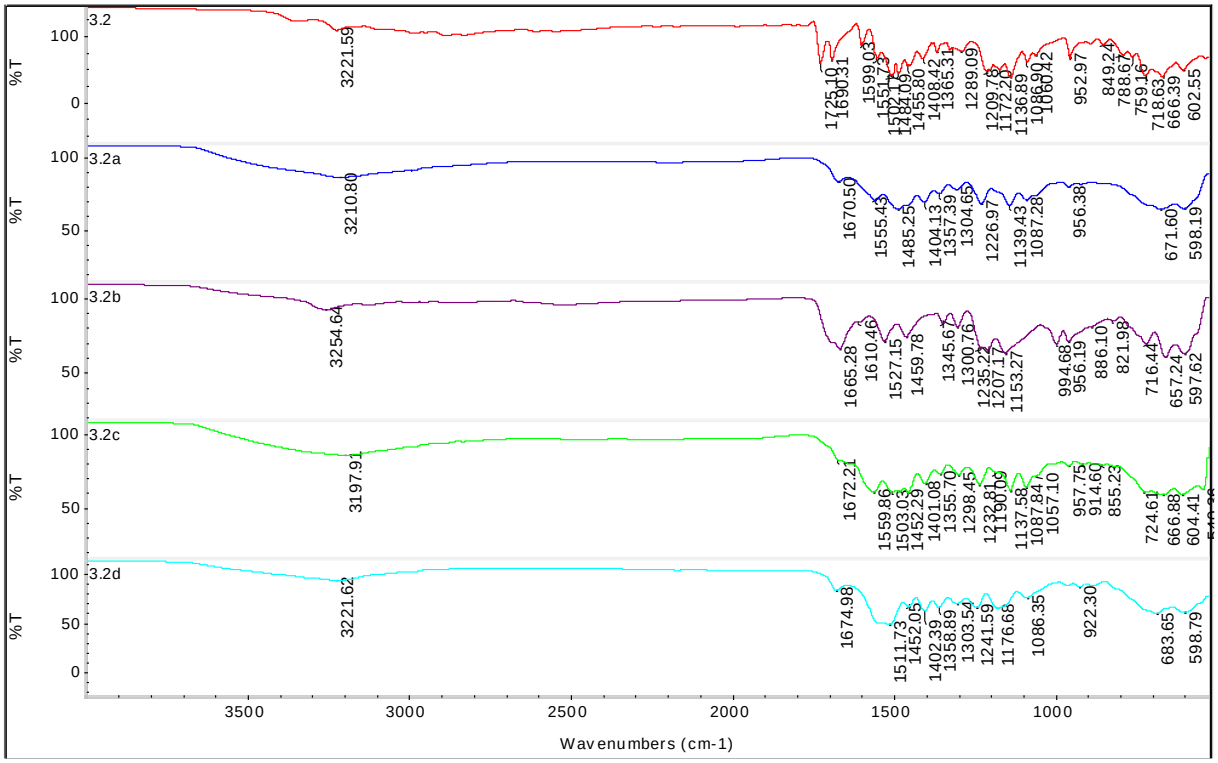

Figure 5. FTIR spectra of metal complexes of compound **3.2**

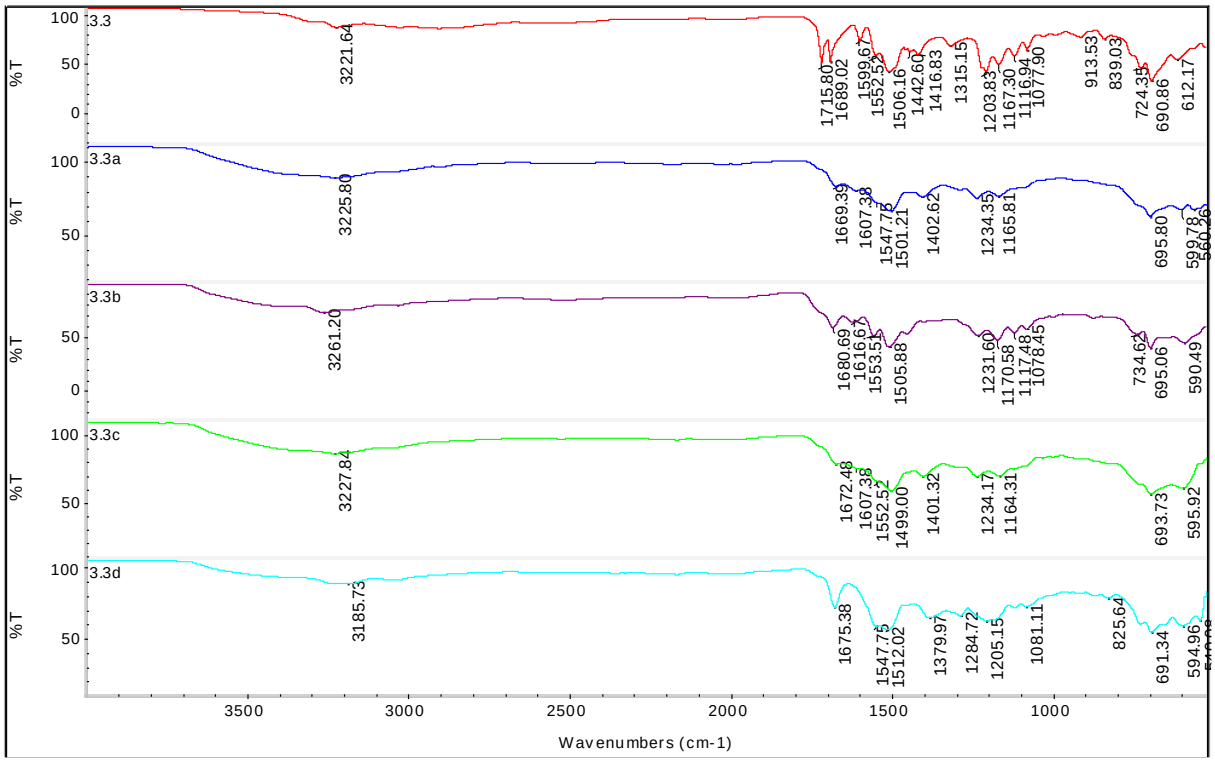

Figure 6. FTIR spectra of metal complexes of compound **3.3**

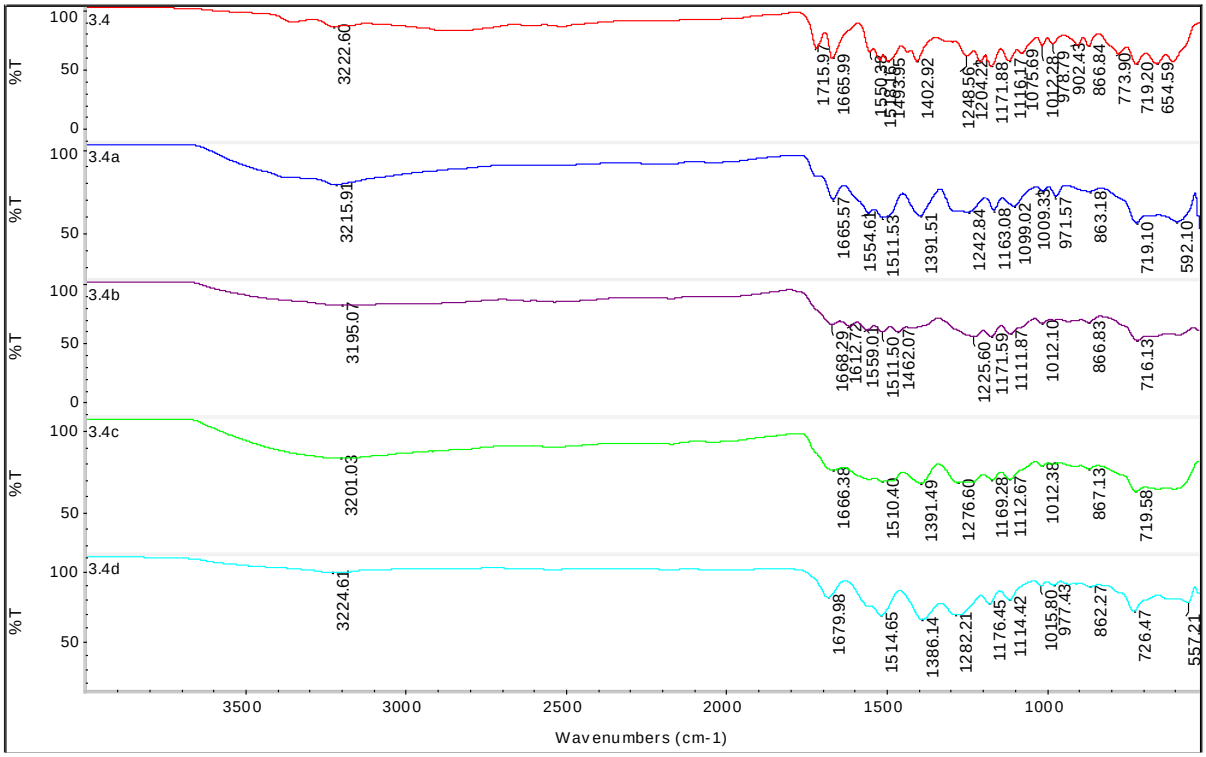

Figure 7. FTIR spectra of metal complexes of compound **3.4**

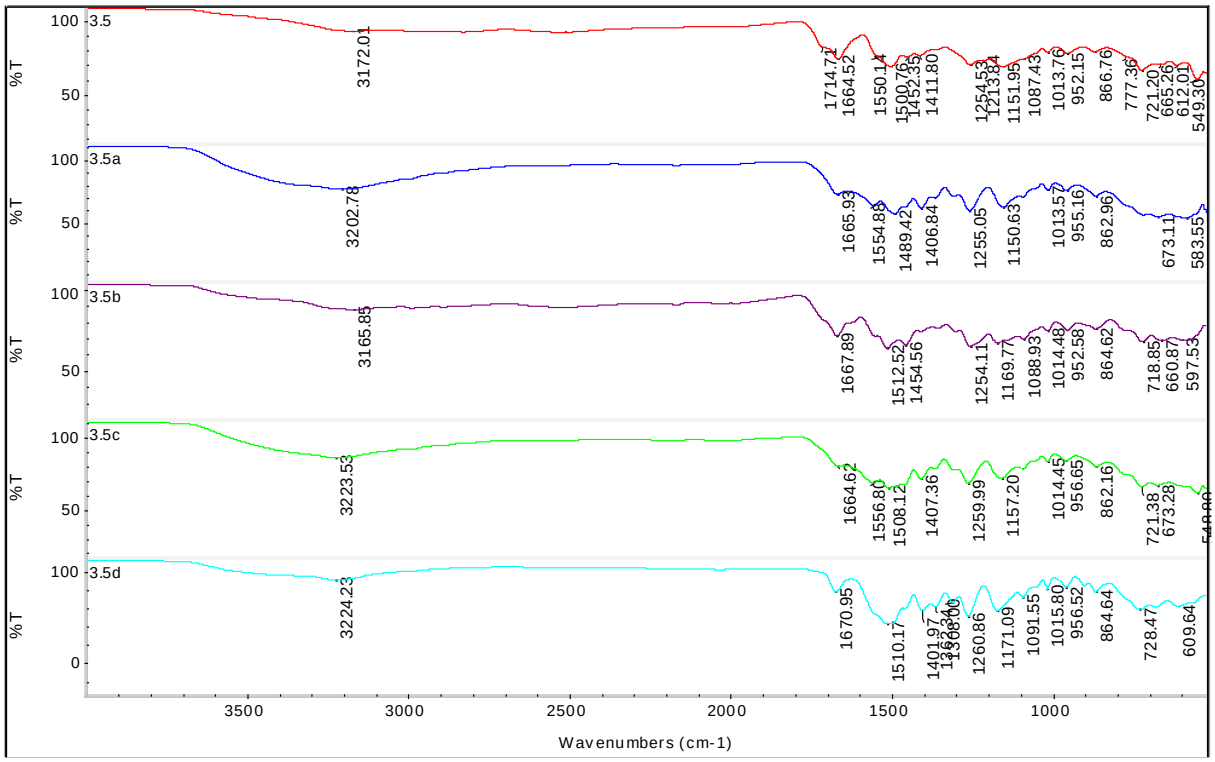

Figure 8. FTIR spectra of metal complexes of compound **3.5**

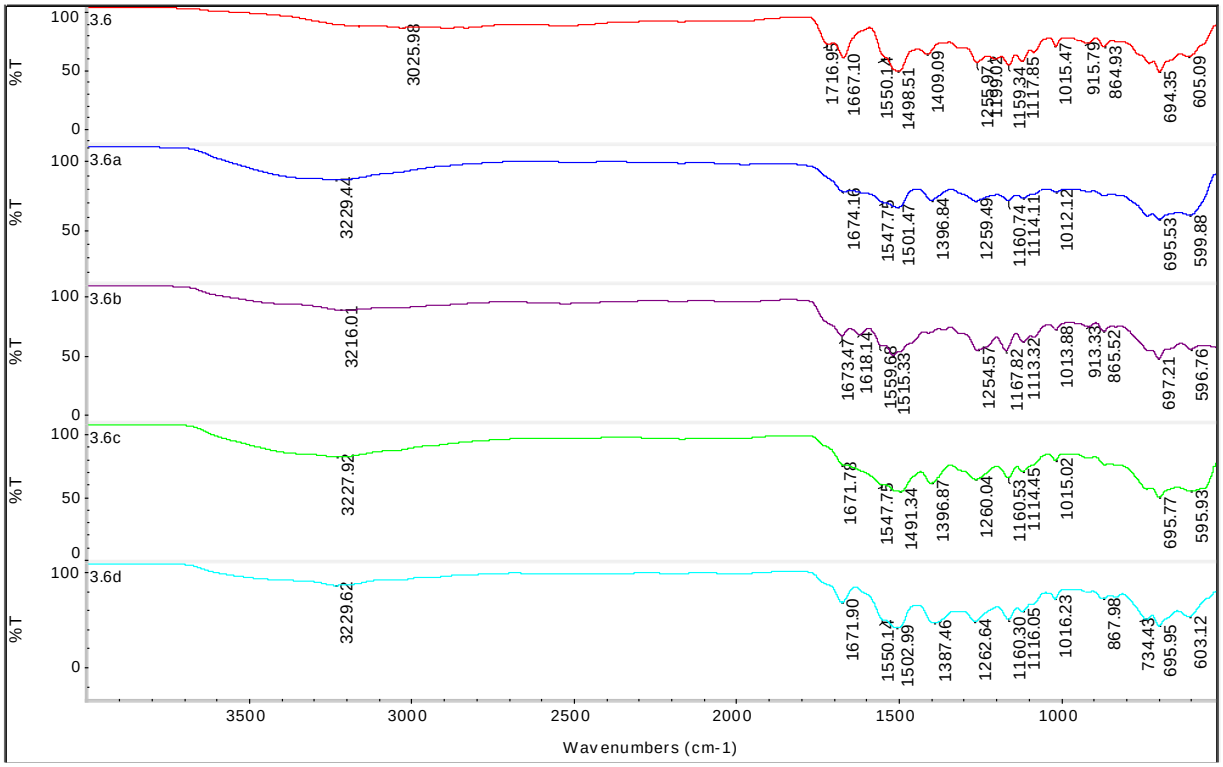

Figure 9. FTIR spectra of metal complexes of compound **3.6**

Table 3. FTIR stretching vibration of compound **3.1(a-d)-3.6(a-d)**

Compound	Wavelength (cm^{-1})			
	v(C=O) carboxylic	*v*(C=O) amide	*v*(C=S)	*v*(C-N)
3.1	1714	1666	1210	1169
3.1a	-	1668	1227	1166
3.1b	-	1674	1228	1178
3.1c	-	1667	1226	1166
3.1d	-	1671	1229	1174
3.2	1725	1690	1210	1172
3.2a	-	1671	1227	1139
3.2b	-	1665	1235	1153
3.2c	-	1672	1233	1138
3.2d	-	1675	1242	1177
3.3	1716	1689	1204	1167
3.3a	-	1669	1234	1166
3.3b	-	1681	1231	1171
3.3c	-	1672	1234	1164
3.3d	-	1675	1205	1152
3.4	1716	1666	1249	1152
3.4a	-	1666	1243	1163
3.4b	-	1668	1226	1172
3.4c	-	1666	1277	1169
3.4d	-	1680	1282	1176
3.5	1715	1665	1255	1152
3.5a	-	1666	1255	1151
3.5b	-	1668	1254	1170
3.5c	-	1665	1260	1157
3.5d	-	1671	1261	1171
3.6	1717	1667	1256	1159
3.6a	-	1674	1259	1161
3.6b	-	1673	1255	1168
3.6c	-	1672	1260	1161
3.6d	-	1672	1263	1160

Anion Addition Studies

Thiourea compounds have been shown to bind anions such as sulphate and carboxylate by forming hydrogen bonds with the anions (Ha *et al.*, 2019). In recent literature, it is shown that some anions can either induce gel-sol transition or sol-gel transition. In the work of Bai and co-workers (2015), the addition of F^- and AcO^- to the hydrazide gels has induced the gel-sol transition due to the disruption of the hydrogen bonding networks by the anions (Bai *et al.*, 2015). Similarly, in our work, we found out that the addition of chloride, fluoride and acetate ions

(as tetrabutylammonium salts) to 50:3 dichloromethane:water mixture gel (**3.5**) also has induced the gel-sol transition as shown in Figure 10.

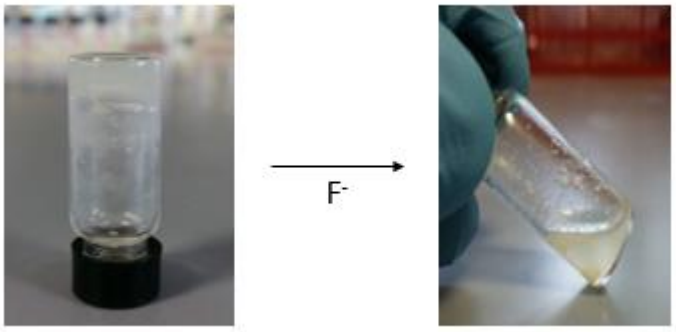

Figure 10. Gel-sol transition due to the addition of tetrabutylammonium fluoride to 50:3 dichloromethane:water mixture gel (**3.5**)

The gel-sol transition of 50:3 dichloromethane:water mixture gel (**3.5**) is possibly due to the disruption of hydrogen bonding between the thiourea molecules (Figure 11) as observed in the previous works of Baddi and co-workers (Baddi *et al.*, 2016). Addition of highly basic anion such as F^- and AcO^- lead to the deprotonation of thiourea NH and cause disruption of hydrogen bonding. In some cases, where the receptor is highly acidic, the deprotonation does not totally take place when only one equivalent of anion is added. In that case, addition of the second equivalent of anion is required to deprotonate the receptor and hence induced the sol-gel transition (Blažek Bregović *et al.*, 2015).

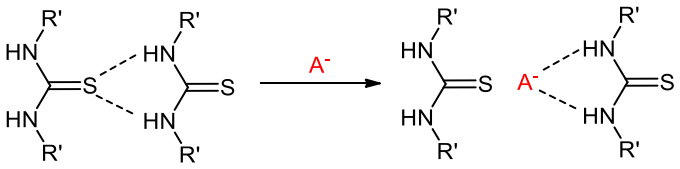

Figure 11. The plausible mechanism of hydrogen bonding disruption of thiourea by anion

Dye Absorption

Apart from cations and anions addition to the gel, we also examined the ability of the gel to absorb organic dyes such as bromocresol green, Eriochrome black-T and xylenol orange. Toxic organic dyes that were disposed into the environmental would cause detrimental effect to human surrounding organisms (Okesola & Smith, 2016). It is widely known that dye molecules can be effectively captured and immobilised in the organogel matrix by self-assembling three-dimensional networks (Liu *et al.*, 2016; Yang *et al.*, 2021). Dye absorption studies were performed on 50:3 dichloromethane:water mixture gel (**3.5**). After 24 hours of contact time, it was found that both Eriochrome black-T and bromocresol green dyes shows gradual increase of absorption in the gel matrix. In contrast, xylenol orange, although it was not absorbed by the gel, it still causes some disruption to the state of the gel as shown in Figure 11. This might be due to the hydrogen bonding interaction that formed between the COOH group of the xylenol orange with the hydrogen bond acceptor units (C=S and C=O) of the gel compound which subsequently compromise the stability of the gel (Panja *et al.*, 2019).

The effectiveness of dye absorption was determined by comparing the absorbance values before and after the addition of dye solution using UV–Vis spectroscopy. The decolorization

of bromocresol green and Eriochrome black-T was consistent with the decreasing in the absorbance values at 400 nm and 517 nm, respectively (Figure 12). Within the first 3 hours, the absorption rates of the bromocresol green and Eriochrome black-T were observed to be at similar rate. However, after 3 hours, the absorption of bromocresol green dye was faster compared to Eriochrome black-T dye. As an anionic dye, both dyes interacted primarily through electrostatic attraction with absorption sites (Yang *et al.*, 2021). It is possible that the difference in absorption capacity between bromocresol green and Eriochrome black-T is attributed to the difference in electrostatic force of attraction between the two compounds towards 50:3 dichloromethane:water mixture gel. Difference in the functional groups of both bromocresol green (-SO_3, -Br and –OH) and Eriochrome black-T (-SO_3, N=N, -NO_2 and –OH) could influence the exchange of electrons between the absorbents and absorbates in addition to the synergetic effect of hydrogen bonding, π-π stacking and acid-base complexes (Yang *et al.*, 2021). The dye absorption rates also could be possibly influence by the length of the molecules (the length of the bromocresol green and Eriochrome black-T is about ±9 Å and ±14 Å, respectively) (Liu *et al.*, 2016). In comparison to prior studies by Khan and co-workers (2019), acid-treated charcoal and additive cobalt acid-treated charcoal absorbs approximately 16.85% and 40.5% of bromocresol dye solution in 12 hours respectively (Khan *et al.*, 2019). Our bisthiourea gel shows better absorption of bromocresol green dye (50%) within 12 hours.

To get an insight on the dye absorption effect on the morphology of 50:3 dichloromethane:water mixture gel, scanning electron microscopy (SEM) has been used to examine the micro-scale structures of the gel after the absorption took place. Figure 13 shows that both dyes cause predominantly interwoven fibrous structures which aggregate together. The width of the fibre after the absorption of bromocresol green and Eriochrome black-T do not shows any drastic change which ranging from 0.17-0.11 µm and 0.18-0.15 µm, respectively. Likewise, Kyzas and co-workers (2015) also observed the same finding in which there is no significant different of SEM images after the absorption of basic dye using grafted chitosan material (Kyzas *et al.*, 2015).

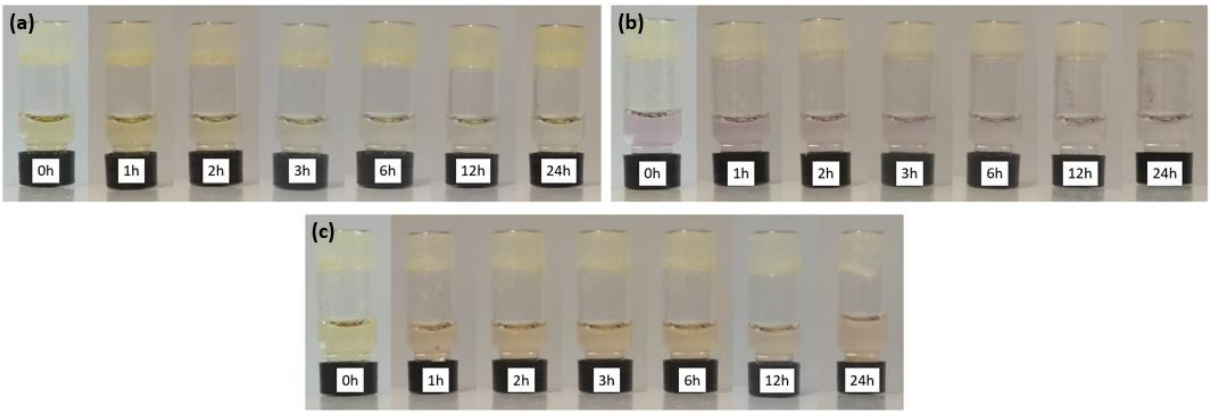

Figure 11. Colour change of (a) bromocresol green, (b) Eriochrome black-T and (c) xylenol orange with respect to the time taken

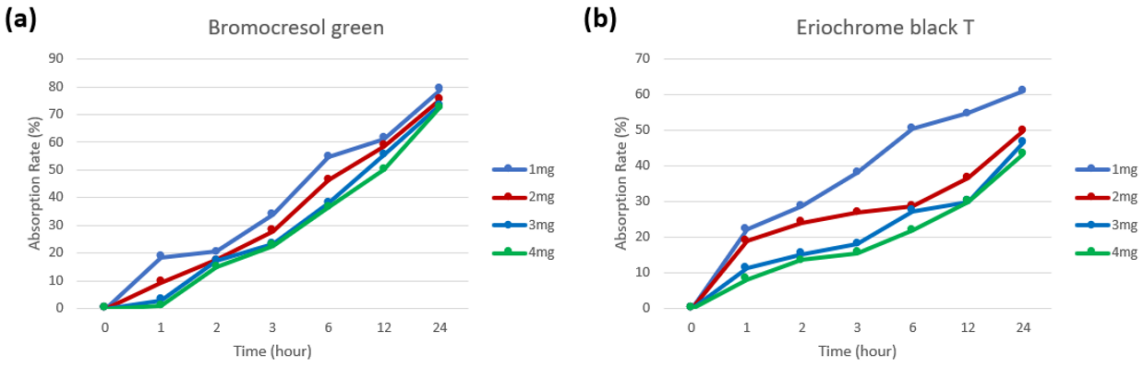

Figure 12. The time (hour) vs. absorption rate (%) of (a) bromocresol green and (b) Eriochrome black-T solution taken after the reaction at 24 hour time interval

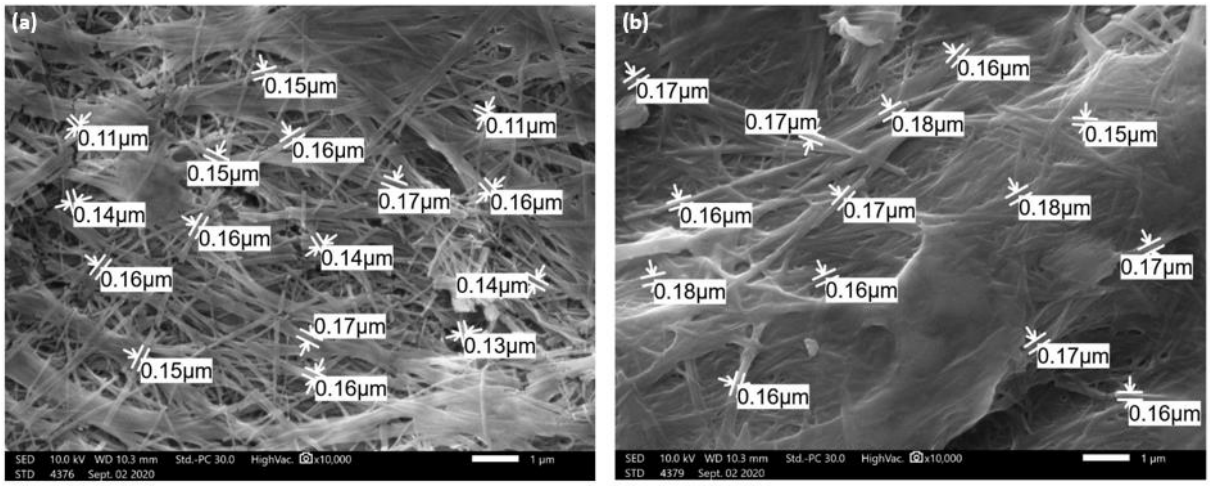

Figure 13. SEM images of gel after the absorption of a) bromocresol green and b) Eriochrome black-T

CONCLUSION

To conclude, bisthiourea derivatives bearing amino acid chains (**3.1–3.6**) have successfully been synthesized and coordinated with $CoCl_2{\cdot}6H_2O$ (**a**), $CuCl{\cdot}2H_2O$ (**b**), $NiCl_2{\cdot}6H_2O$ (**c**) and $Pb(NO_3)_2$ (**d**) to form complexes **3.1(a-d)-3.6(a-d)**. Bisthiourea compound, **3.5** has been shown to form a thermoreversible gel in 50:3 dichloromethane:water mixture at minimum gel concentration of 0.5%. In contrast, the addition of cations such as Co^{2+}, Cu^{2+}, Ni^{2+}, Pb^{2+} did not induce the formation of metallogel. Addition of anions F^-, AcO^- and Cl^- as tetrabutylammonium salts induced the gel-sol transition due to the disruption of hydrogen bonding between the sulfur and hydrogen atoms in the compound. The dichloromethane:water gel of **3.5** showed excellent absorption of organic dyes, bromocresol green and Eriochrome black-T with the percentage of absorption at 75% and 61%, respectively after 24 hours. The good dye absorption properties of bisthiourea gel have shown promising potential for the development of environmental pollutants absorbents.

ACKNOWLEDGEMENTS

The work was financially supported through a financial grant supported by Universiti Malaysia Sarawak (F07/SpMYRA/1713/2018).

REFERENCES

Bachl, J., Sampedro, D., Mayr, J. & Diaz Diaz, D. (2017). Ultrasonication-enhanced gelation properties of a versatile amphiphilic formamidine-based gelator exhibiting both organogelation and hydrogelation abilities. *Physical Chemistry Chemical Physics*, 19(34): 22981–22994.

Baddi, S., Madugula, S.S., Sarma, D.S., Soujanya, Y. & Palanisamy, A. (2015). Combined experimental and computational study of the gelation of cyclohexane-based bis(acyl-

semicarbazides) and the multi-stimuli-responsive properties of their gels. *Langmuir*, 32(3): 889–899.

Bai, B., Mao, X., Wei, J., Wei, Z., Wang, H. & Li, M. (2015). Selective anion-responsive organogel based on a gelator containing hydrazide and azobenzene units. *Sensors and Actuators B: Chemical*, 211: 268–274.

Blažek Bregović, V., Basarić, N. & Mlinarić-Majerski, K. (2015). Anion binding with urea and thiourea derivatives. *Coordination Chemistry Reviews*, 295: 80–124.

Cao, X., Zhao, N., Lv, H., Gao, A., Shi, A., & Wu, Y. (2018). 4-Nitrobenzene thiourea self-assembly system and its transformation upon addition of Hg^{2+} ion: Applications as sensor to fluoride ion. *Sensors and Actuators, B: Chemical*, 266: 637–644.

Cheng, N., Kang, Q., Xiao, J., Du, N. & Yu, L. (2018). Supramolecular gels: using an amide-functionalized imidazolium-based surfactant. *Journal of Colloid and Interface Science*, 511: 215–221.

Chetia, M., Debnath, S., Chowdhury, S. & Chatterjee, S. (2020). Self-assembly and multifunctionality of peptide organogels: Oil spill recovery, dye absorption and synthesis of conducting biomaterials. *RSC Advances*, 10(9): 5220–5233.

Christoff-tempesta, T., Lew, A. & Ortony, J. (2018). Beyond Covalent Crosslinks: Applications of Supramolecular Gels. *Gels*, 4(2): 1–40.

Dastidar, P., Ganguly, S. & Sarkar, K. (2016). Metallogels from Coordination Complexes, Organometallic, and Coordination Polymers. *Chemistry - An Asian Journal*, 11(18): 2484–2498.

De, A. & Mondal, R. (2018). Toxic Metal Sequestration exploiting an unprecedented low-molecular-weight hydrogel-to metallogel transformation. *ACS Omega*, 3(6): 6022-6030.

Fakhar, I.M., Yamin, B. & Hasbullah, S.A. (2016). Synthesis and characterization of bis-thiourea having amino acid derivatives. *American Institute of Physics*, 1784(1): 1–7.

Ha, S., Lee, J., Kim, K.S., Choi, E. J., Nhem, P. & Song, C. (2019). Anion-responsive thiourea-based gel actuator. *Chemistry of Materials*, 31(15): 5735–5741.

Han, L., He, Y., An, R., Wang, X., Zhang, Y., Shi, L. & Ran, R. (2019). Mussel-inspired, robust and self-healing nanocomposite hydrogels: Effective reusable absorbents for removal both anionic and cationic dyes. *Colloids and Surfaces A*, 569: 18–27.

Hooper, A.E., Kennedy, S.R., Jones, C.D. & Steed, J.W. (2016). Gelation by supramolecular dimerization of mono(urea)s. *Chemical Communications*, 52(1): 198–201.

Khan, I., Ur Rahman, N., Ali, A. & Saeed, K. (2019). Adsorption of cobalt onto activated charcoal and its utilization for decolorization of bromocresol green dye. *Bulgarian Chemical Communications*, 51(4): 488–493.

Kyzas, G. Z., Siafaka, P. I. Pavlidou, E. G., Chrissafis, K. J., & Bikiaris, D. N. (2015). Synthesis and adsorption application of succinyl-grafted chitosan for the simultaneous removal of zinc and cationic dye from binary hazardous mixtures. *Chemical Engineering Journal*, 259: 438–448.

Li, L., Zhou, N., Kong, H. & He, X. (2019). Controlling the supramolecular polymerization and metallogel formation of Pt(II) complexes via delicate tuning of non-covalent interactions. *Polymer Chemistry*, 10(40): 5465–5472.

Liu, J., Xu, F., Sun, Z., Pan, Y., Tian, J., Lin, H.C. & Li, X. (2016). A supramolecular gel based on a glycosylated amino acid derivative with the properties of gel to crystal transition. *Soft Matter*, 12(1): 141–148.

Liu, Y., Wang, Y., Jin, L., Chen, T. & Yin, B. (2016). MPTTF-containing tripeptide- based organo gels: receptor for 2,4,6-trinitrophenol and multiple stimuli-responsive properties. *Soft Matter*, 12(3): 934–945.

Mondal, S. & Dastidar, P. (2018). Mixed ligand coordination polymers for metallogelation and iodine adsorption. *Crystal Growth and Design*, 19(1): 470-478.

Okesola, B.O. & Smith, D.K. (2016). Applying low-molecular weight supramolecular gelators in an environmental setting-self-assembled gels as smart materials for pollutant removal. *Chemical Society Reviews*, 45(15): 4226–4251.

Panja, A. & Ghosh, K. (2018). Diaminomalenonitrile -decorated cholesterol -based supra molecular gelator: aggregation, multiple analyte (hydrazine, Hg^{2+} and Cu^{2+}) detection and dye adsorption. *New Journal of Chemistry*, 42(16): 13718–13725.

Panja, A., Ghosh, S. & Ghosh, K. (2019). A sulfonyl hydrazine cholesterol conjugate: gelation, anion interaction and its application in dye absorption. *New Journal of Chemistry*, 42: 10270–10277.

Sengupta, S., Goswami, A. & Mondal, R. (2014). Silver-promoted gelation studies of an unorthodox chelating tripodal pyridine-pyrazole-based ligand: Templated growth of catalytic silver nanoparticles, gas and dye adsorption. *New Journal of Chemistry*, 38(6): 2470–2479.

Staicu, T., Iliş, M., Cîrcu, V. & Micutz, M. (2018). Influence of hydrocarbon moieties of partially fluorinated *N*-benzoyl thiourea compounds on their gelation properties. A detailed rheological study of complex viscoelastic behavior of decanol/*N*-benzoyl thiourea mixtures. *Journal of Molecular Liquids*, 255: 297–312.

Tatikonda, R., Bhowmik, S., Rissanen, K., Haukka, M. & Cametti, M. (2016). Metallogel formation in aqueous DMSO by perfluoroalkyl decorated terpyridine ligands. *Dalton Transactions*, 45(32): 12756–12762.

Wezenberg, S.J., Croisetu, C.M., Stuart, M.C.A. & Feringa, B.L. (2016). Reversible gel-sol photoswitching with an overcrowded alkene-based bis-urea supergelator. *Chemical Science*, 7(7): 4341–4346.

Yang, Z., Wu, G., Gan, C., Cai, G., Zhang, J. & Ji, H. (2021). Effective adsorption of arsenate, dyes and eugenol from aqueous solutions by cationic supramolecular gel materials. *Colloids and Surfaces A: Physicochemical and Engineering Aspects*, 616: 126238.